DR VICTOR J. RICO (Orcid ID : 0000-0002-5083-0390)

DR FRANCISCO REY-GARCÍA (Orcid ID : 0000-0002-3083-9355)

Article type : Article

Laser induced coloration of ceramic tiles covered with magnetron sputtered precursor layers

V. J. Rico[1]*, R. Lahoz[2]*, F. Rey-García[3, 4], I. de Francisco[3], J. Gil-Rostra[1], J.P. Espinós[1], G. F. de la Fuente[3]*, A.R. González-Elipe[1]

[1] Instituto de Ciencia de Materiales de Sevilla (CSIC-Univ. Sevilla). Avda. Américo Vespucio 49. 41092 Sevilla. Spain.

[2] Centro de Química y Materiales de Aragón (CSIC-Univ. Zaragoza). María de Luna, 3. 50018 Zaragoza. Spain

[3] Instituto de Ciencia de Materiales de Aragón (CSIC-Univ. Zaragoza). María de Luna, 3. 50018 Zaragoza. Spain

[4] Departamento de Física & I3N, Universidade de Aveiro, 3810-193 Aveiro, Portugal

E-mail address: victor@icmse.csic.es

E-mail address: rlahoz@unizar.es

E-mail address: german.delafuente.leis@csic.es

Keywords

Decorative coating, magnetron sputtering, ceramic tiles, laser processing, laser furnace, surface plasmon resonance.

Abstract

This paper reports a new methodology for the coloring of glazed ceramic tiles consisting of the near infrared pulsed laser processing of copper containing oxide coatings prepared by magnetron sputtering. As a second approach, the employ for the same purpose of a novel laser furnace technique is also described. Changing the laser parameters and using the laser furnace to treat the tiles at high temperature during irradiation has resulted in a wide color palette. The optical characterization of the modified tiles by UV-Vis spectroscopy has been complemented with their microstructural and compositional analysis by Scanning Electron Microscopy (SEM), Transmission Electron Microscopy (TEM) and Time of Flight Secondary Ion Mass Spectrometry. The chemical composition of the surface was obtained by X-ray photoemission (XPS) and its structure determined by XRD. The chemical resistance was characterized by several tests following the norm ISO 10545-13. Color changes have been attributed to surface microstructural and chemical transformations that have been accounted for by simple models involving different ablation, melting, diffusion and segregation/agglomeration phenomena depending on the laser treatments employed.

Introduction

The fabrication of colored tiles is a key process for the production of decorative products of high commercial demand of the ceramic industry. [1-3] Typical coloration methods in metal-decorated ceramic tiles are based on surface plasmon resonance effects, which entail the promotion of solid state reactions producing the reshaping of metal nanoparticles or chemical changes in the metal phase. [4-7] Successful examples of this approach using thermal annealing procedures have been reported in the literature and applied in the industry. Improvements on this methodology have pursuit decreasing the temperature to obtain the pigments,[8] to use other strategies based on the ink-jet printing technology or the employ of nano or sub-micron pigments and "ceramic inks". [9] Laser processing at room temperature (i.e. avoiding costly thermal processes) have been also proposed as a suitable methodology to modify the surface aspect of ceramic materials. [10, 11] A typical procedure consists of the lithographic ablation of metal films according to specific designs. [12, 13] Laser induced solid-state reactions between a coating layer and a ceramic substrate has been also proposed as a way of inducing tile coloration. For example, we have recently reported a hybrid methodology that combines the physical vapor evaporation of copper films and their treatment with a near infrared laser (NIL) to induce a specific coloring of tiles. [14]

A common shortcoming by the NIL treatment of metal films is the reflection of laser beams by mirror-like surfaces. This problem was avoided in our previous work utilizing as dispersive centers nanoparticulated films prepared by electron beam evaporation at oblique angles.[15] In the present work we explore a new coloring methodology that entails the NIL treatment of ceramic tiles covered by SiO_2-copper oxide coatings deposited by magnetron sputtering (MS). MS is an effective thin film deposition technique widely used in the industry to cover large areas (e.g., in flat glass manufacturing) and that, therefore, can be quite straightforward for ceramic tiles.[16] Unlike the small amount of metal utilized in our previous work to avoid laser reflection effects, the present procedure relying on non-reflective coatings is not limited by the thickness of the deposited copper oxide. To enhance the stability of the coating and to decrease the costs associated to this relatively expensive metal, copper has been diluted within a matrix of SiO_2, an oxide easily miscible with other ceramic components, particularly in tile substrates with a $ZrSiO_4$ composition as in the present study. This affinity also ensures similar thermal expansion coefficients and eludes the necessity of an additional interface or buffer layer. MS deposition of transition metal oxides diluted in SiO_2 matrix thin films has been previously used for the fabrication of colored ophthalmic coatings.[17] Herein, to tailor the final color aspect of the tiles, we firstly essay NIL treatment at room temperature of these Cu-Si mixed oxide layers deposited on the ceramic tiles. In a second approach we used a continuous CO_2 laser incorporated in a laser furnace set-up.[18, 19] In comparison with conventional thermal procedures for processing ceramic, bricks and similar materials, this laser-furnace method is advantageous because processing temperatures can be relatively lower and can provide alternative finishing effects.[20] Overall, the wide range of colors obtained in this work proves the feasibility of using laser induced solid-sate reactions between oxide layers and tile substrates for endowing new aesthetic effects to ceramic materials.

Experimental

Copper dissolved in silica glass were prepared by reactive MS co-deposition. The experimental set-up (see Figure 1) consisted of a vacuum chamber equipped with two magnetron sputtering sources, for silicon (p-type, Kurt Lesker 99.99%) and for copper (Kurt Lesker 99.95%), with diameters of 3 and 2 inches respectively, a rotatable sample holder (4 inches of diameter), a quartz crystal monitor to control the deposition rates and a couple of mass flow controllers to adjust the O_2/Ar mixture of the plasma discharge.

Si and Cu magnetron sources were operated with two pulsed DC power supplies (AE Pinnacle Plus+) applying a power of 300 W and 50 W, respectively (frequency 120 KHz, reverse time 2.5 µs). The base pressure of the system was 2.0 10^{-7} mbar. The process gas consisted of a mixture of Ar (15 sccm) and O_2 (15 sccm) at a pressure of 5.0 10^{-3} mbar. To ensure thickness and composition homogeneity over the whole substrate area, the two MS sources were directed towards the center of a rotating holder (tilted geometry, 60º vs. normal). The rotation speed of the sample holder was fixed at 30 rpm, and the distance between the substrates and the MS sources was 15 cm. The samples were prepared at room temperature although, during film growth, substrates can reach up to 50 ºC due to ion/electron impingement. Thickness of deposited copper dissolved in silica films was controlled during deposition by a quartz crystal monitor situated at normal geometry with respect to the targets. The measured deposition rate was 4.5 nm/min, and the film thickness 500 nm. The thin films were flat and homogeneous and consisted of a homogeneous distribution of copper oxide within a SiO_2 matrix. These layers did not present a mirror like behavior and were therefore well suited for treatment with NIL beams.

Reference samples were prepared on quartz and silicon flat substrates. Pieces of quartz plates were used for the transmission UV-vis characterization of the mixed oxide coatings, while Si (100) wafers were used for the observation of the “as deposited” thin films by scanning electron microscopy (SEM). Similar mixed oxide thin films were simultaneously deposited on commercial tile substrates with a glaze composition based on $ZrSiO_4$ (confirmed by the measurements of XRD shown in the Supporting information S1) provided by TORRECID Group, S. L. with size 40 x 40 mm^2.

The coated samples were treated with either a diode pumped solid-state nanosecond Nd:YVO_4 laser (Powerline E20, Rofin) or a diode pumped fiber Yb:YAG laser (Easy Mark 20, Jeanologia), both emitting at a wavelength of 1064 nm.[14] The two lasers were provided with a galvanometer beam steering system and a flat-field lens of 160 mm focal distance giving a spot size of ca. 26 microns, respectively. Lasers were operated in the pulsed mode at repetition rates varying from 0 to 150 kHz, output power values from 1.10 to 20 W and pulse widths from 50 to 220 ns. Irradiation experiments were carried out in air and under vacuum conditions. Although various parameters were changed in a thorough parametric analysis of laser operation (e.g., power, pulse duty cycle, air and vacuum conditions, among others), the irradiance varying from 0.001 to 15 MW/cm^{-2} was taken as the relevant magnitude to account for the observed coloration effects. Samples were moved during the treatment at a rate of 0.10 mm/s, while the laser beam was scanned perpendicular to the movement direction at a rate of 500 mm/s. Table 1 summarizes the different conditions utilized for the preparation of tile samples M0 to M3 taken as representative of the color changes induced by NIL treatment.

In another set of experiments, laser surface irradiation was carried out in a Laser-Furnace system consisting of a continuous ceramic roller furnace, where a continuous wave (cw) CO_2 laser (Rofin DC025 SLAB CO_2), emitting at 10.6 μm wavelength with a maximum nominal output power of 2 kW, reached the sample through an upper slot [18]. In the laser-furnace system, samples moved at constant rate into the continuous roller furnace in an orthogonal direction to the laser line focus. The temperature in the roller furnace was adjusted to 893 K, a value that was deemed sufficient to avoid crack formation. Sample M4 was prepared by moving the coated tiles through the continuous roller furnace at a displacement rate of 7000 mm h^{-1} in the absence of any laser irradiation. Sample M5 was prepared under laser irradiation by focusing the beam onto the sample surface through an optical galvanometer head that transformed the circular cross-section beam into a line of approx. 0.8 mm in thickness (laser spot diameter) and a width of 620 mm. The beam scanning rate was 27 mm s^{-1}and the laser emission power 500 W (c.f., Table 1). A table including all NIL and CO_2 laser parameters is presented as Supporting Information S2.

UV-Vis-NIR (near infrared) Spectroscopy (Pelkin-Elmer Lambda 750 S) in transmission mode was used for the characterization of quartz plates, while the reflection mode was used to assess the optical behavior of ceramic tile samples before and after laser irradiation. For these measurements, samples were placed in the front window of the integration sphere of the spectrometer. Color coordinates (i.e., Hunter´s parameters) were deduced from these spectra using the usual transformation procedure. [21]

Microstructural characterization was carried out by means of a Talos FEI transmission electron microscope equipment working at 200 KV both for TEM images and the STEM measurements and composition mappings. Scanning electron microscopy (SEM) analysis of the samples was carried out in a Hitachi S4800 field emission microscope.

Depth profiles of the differently treated tile samples were obtained in a Time of Flight Secondary Ions Mass Spectrometer (TOF-SIMS) using an instrument from Ion-ToF GmbH, Germany. The samples were bombarded with a pulsed bismuth ion beam. The generated secondary ions were extracted by applying a 10 kV voltage and their time of flight from sample to detector was measured using a reflection mass spectrometer. Typical analysis conditions entailed a 25 keV pulsed Bi^+ ion beam rastered over a 500x500 mm^2 area and impinging at 45º incidence. An electron flood gun for charge compensation was used during the measurements. Peak intensities were normalized to the total ion intensity.

X-ray photoelectron spectra were recorded in the pass energy mode in a PHOIBOS 100DLD (SPECS) using the Mg Kα line as excitation source. The energy scale of the spectra was referred to the C1s line at 284.5 eV for the adventitious carbon contaminating the surface of the samples. Cu/Si atomic ratios were determined from the areas of the Cu2p and Si2p photoemission lines normalized by their corresponding sensitivity factors.

X-ray diffraction (XRD) analysis was carried out in a Siemens D5000 diffractometer working in grazing configuration at 5º. Data supported the amorphous character of the deposited upper layers before and after laser treatment. The tile substrate was examined with the same apparatus working in a Bragg-Brentano configuration to probe not only its surface layers but the whole thickness of the glaze.

Determination of the chemical resistance was done using immersion tests on acids and basis with different concentrations and times of treatment according to the norm ISO 10545-13.

Results and Discussion

Copper dissolved in silica glass and precursor ceramic samples

The reference copper dissolved in silica glass layers, deposited on quartz, depicted a well-defined greenish color that can be accounted for by the formation of a solid solution of copper cations within a SiO_2 network [17]. The UV-vis spectrum of this layer reported in Figure 2 presents a low and broad absorption band centered around 650 nm which is superimposed on the typical interference oscillatory shape of a transparent thin film of several hundred nm. This band can be attributed to the absorption of copper cations in copper oxide enriched clusters dispersed within the SiO_2 matrix.[22] Its position suggests that the majority of copper is in the form of Cu^{2+} species,[4] an assignment that coincides with X-ray absorption results reported in a previous work [17]. The SEM analysis of this reference sample confirmed the formation of a homogenous and dense thin film as shown in the left side on the inset in Figure 2. The cross-section micrograph in this inset was obtained by TEM and shows that the thickness of this film was approximately 500 nm. Moreover, the higher magnification micrograph shown in the inset of Figure 2 shows that clusters enriched in copper oxide, characterized in the image by a higher intensity of brightness, have a size of around 5-10 nm.

The as prepared coated tile samples (i.e., sample M0 in Table 1) depicted an intense and broad absorption band with a minimum between 650-700 nm (Figure 3a)) that, in agreement with the previous assignment in the reference quartz sample, can be associated to a broad dispersion of copper oxide clusters distributed within a SiO_2 matrix.[22] As a result, sample M0 presented a dark green color similar to that of the coating deposited on quartz (see Hunter´s parameters in Table 1). SEM characterization of this sample (Figure 3b)-left) revealed a similar topography where copper enriched clusters with a size of ca. 30 nm can be identified.[17] A first evaluation of the TOF-SIMS depth profiles of sample M0 (Figure 3c)-top) confirms that a homogeneous in depth Cu-Si oxide layer was covering the tile substrate. This depth profile provided a first calibration of the sputtering etching rate of the coating and substrate systems that was taken as a time-scale reference for the analysis of the laser treated samples (i.e., the 500 nm thickness of the Cu-SiO_2 layers corresponds to approximately 900 seconds of sputter etching, time at which the Cu^+ TOF-SIMS signal drops abruptly and the Zr^+ signal rises). The complete coverage of the tile substrate by the copper-silicon oxide coating was confirmed by XPS: Cu and Si signals with no observable Zr peak characterized the spectrum of this sample where a Si/Cu atomic ratio of 27 was obtained from the area of the Cu2p and Si2p peaks (c.f., Table 1). Analysis of the spectral zones of copper in Figure 4 also revealed that copper is in the form of Cu^{2+} [14] as proven by the shape of the Cu2p and CuLMM bands and a value of the measured Auger parameter of 1850.6 eV (for a more detailed discussion of Auger parameter concept and its calculation, see ref [23] and the supporting information S3).

Laser irradiation of coated tiles

Laser irradiation of coated tile samples rendered different colors and Hunter´s parameters as summarized in Table 1, where the laser irradiance values used to obtain the most intense and homogeneous coloration are also included (see Table S2 in supporting information for a complete account of the laser parameters used). The processing methods herewith presented are scalable and highly reliable, as they are based on commercial galvanometer scanning mirror technology, widely available and industrially mature. These scanning devices enable full control of laser energy coupling onto surfaces, as well as scanning of large areas. XPS, UV-vis, SEM and SIMS analysis of the M1-M5 samples was used to determine the surface changes experienced by the laser treated samples. These changes will be discussed in terms of different phenomena such as ablation, melting or surface segregation of copper clusters or copper partial coverage by melted and segregated material from the tile substrate. Most important for potential applications of these laser treatments is their high chemical stability as proved with standardized tests with acids (see supporting information S4).

Irradiation at room temperature with pulsed NILs was carried out varying different parameters. The obtained effects will be illustrated here with results corresponding to three different values of irradiance at a temperature of 298 K (i.e., corresponding to samples M1, M2 and M3 in Table 1). The interaction of this type of pulsed laser beams with oxide materials are known to induce heating, melting and diffusion of species, as well as ablation and redeposition processes that lead to changes in the composition and microstructure of the outer layers. As a result of this series of phenomena the modified layers form a continuum with the glaze substrate, avoiding any adhesion or delamination problem. The existence of ablation processes during the laser treatments at the high irradiance values utilized for samples M1 and M2 was supported by the observation of plasma plumes [24] that were particularly intense when performing the experiments in vacuum. The UV-vis-NIR spectrum in Figure 3 corresponding to sample M1, prepared at the highest irradiance conditions, is characterized by a high reflectance in the NIR region, a continuous decreasing reflectance in the visible region and a narrow absorption band at 595 nm. The relatively small reflectance at low wavelengths must be at the origin of the grey color of this sample and of the metallic lustre that could be observed when looking to it at grazing angles. The narrow feature in the spectrum can be attributed to surface plasmon resonance (SPR) absorption by Cu^0 nanoparticles [25] likely covered by an oxide outer layer.[4] A similar coloration effect induced by laser treatment was found in previous work using a metal nanoparticulate film as precursor layer.[14] The aspect changes experienced by sample M1 were accompanied by important modifications in its surface microstructure.[26] The SEM micrograph in Figure 3b)-right reveals a rather rough surface where a dendritic enrichment in higher atomic mass atoms (bright SEM areas) can be observed. Meanwhile, the TOF-SIMS analysis of this sample (Figure 3c)-bottom) shows that the laser treatment had blurred the layer structure characteristic of sample M0 and transformed it into a rather homogeneous in-depth distribution of Zr (from the substrate) and Si species. In addition, this profile shows that copper nanoparticles are confined at the topmost surface layers of samples. All these changes support a considerable ablation removal of copper (and likely silicon) from the Cu-SiO_2 film, a process that would be accompanied by the redistribution of the remaining copper clusters within a mixed ZrO_2 (from the substrate) and SiO_2 (from substrate and/or coating) matrix. Under these conditions the observed chemical reduction of copper must be attributed to the high local temperatures and the ablation loss of oxygen induced during irradiation. It is noteworthy that similar results were obtained when performing the experiment either in air or in vacuum, which supported the fact that air does not prevent the reduction of the copper remaining in the upper surface layers of the tiles.

The Si/Cu ratio of 5.3 determined by XPS for this sample (Figure 4 and Table 1) is smaller than that found in sample M0 (i.e. Si/Cu ratio of 27), in agreement with the evidence provided by TOF-SIMS of a copper enriched outer layer. Furthermore, the shape of the Cu2p and CuLMM spectra and the Auger parameter values determined for sample M1 (see supporting information S3) confirm that copper at the surface is in the form of Cu^0 (1851.2 eV), Cu^+ (1847.2 eV) and Cu^{2+} (1850.8 eV) species, whereby the observed enrichment in Cu^+ must result from metallic copper particles exposed to the air and/or partially covered or in contact with SiO_2/ZrO_2. [23]

Sample M2 obtained at intermediate laser irradiances presented a grey color and a highly reflective surface, particularly in the NIR region. The SEM micrograph of this sample in Figure 5b)-left reveals an inhomogeneous surface where agglomerates with two size distributions of 100 nm and 30-50 nm can be identified. Meanwhile, the TOF-SIMS in-depth analysis in Figure 5c)-top shows that copper, distributed through a depth of approximately 150 nm, is enriched at the surface, its concentration decreasing smoothly in depth. In parallel, the Zr signal increases to a maximum when copper presents its minimum (around 130 nm in depth). Meanwhile, silicon appears rather homogenously distributed in depth. This surface profile supports the partial ablation removal of the Cu-SiO_2 thin film and a partial reduction of copper similar to that observed in sample M1. However, unlike sample M1, copper does not appear confined at the most external surface layers but distributed through a depth of ca. 130 nm. This depth profile renders a Si/Cu XPS surface ratio of 8.6, while the Cu2p and Cu LMM spectra in Figure 4 support that copper at the surface is in the form of Cu^{+} (1847.6 eV) and Cu^{2+} (1850.2 eV) species with a greater contribution of Cu^{2+} than in sample M1. These XPS results strongly suggest that clusters observed in the SEM image of sample M2 are surface oxidized.

Sample M3 was prepared at low laser irradiance. Its UV-vis-NIR spectrum (c.f., Figure 5a)) depicts a continuous yet decreasing reflection extending through the visible and NIR spectral regions and an absorption edge at around 750 nm responsible for the yellow-orange color of this sample. This absorption edge can be associated to the convolution of absorptions due to Cu_2O (band gap of 2,17 eV) and CuO (band gap of 1,2 eV) [4]. The SEM micrograph of this sample in Figure 5b)-right reveals a melted surface with holes of approximately 100 nm. This microstructure suggests that, at the low irradiance values utilized in this experiment, ablation was less important than in samples M1 and M2 and that laser irradiation induced other effects such as surface heating, melting and enhanced diffusion of species.

Differences between samples M1/M2 on the one side, and M3 on the other, can be rationalized in the following terms. Intense surface interaction above a certain laser irradiance threshold, induces vigorous evaporation of SiO_2 via suboxide formation.[27]

$$SiO_2 \rightarrow SiO + \tfrac{1}{2} O_2$$

In addition, other silicate components within the ceramic glaze may also decompose in a similar fashion.[27] Such thermodynamically favored vigorous decomposition of silica and silicate components may not only contribute to the formation of observable intense plasma plumes, but must also result in our case in the observed copper enrichment in the remaining substrate surface layers. In addition, the mechanical shock waves associated to plasma formation must also affect the final surface morphology due to their interaction with the melt below.[12, 26, 28] Very likely, this was a critical factor leading to the rough surface morphology, typical of ns regime ablation, which is a characteristic of samples M1 and M2. On the other hand, the lower irradiance level used in sample M3 should entail a decrease in the ablation contribution and an enhancement of melting due to the contribution of other laser irradiation components. The irradiance level is known to cause a direct instant melting at and around the laser focal spot, while the pulse repetition rate, in the case of pulsed irradiation, is known to produce melting via energy incubation[26, 28] (i.e., as the pulse repetition rate increases, so does the melt volume). These phenomena may explain the differences encountered between samples M2 and M3, where the increase in pulse repetition rate (from 100 to 150 kHz, see Table S2) produces a decrease in energy per pulse (lower irradiance) and an increase in energy incubation, both favoring melting over ablation and contributing in sample M3 to increase the thermal diffusion and the mixing of species at the interface [28]. This view was confirmed by the observation in this sample of a smooth melted surface and a rather homogeneous in-depth distribution of species as determined by TOF-SIMS. In fact, Figure 5c)-bottom shows that copper is depleted at the upmost zone of the sample where Si replaces it. Then, enrichment of both copper and silicon (this latter smoothly decreasing) occurs up to a depth of approximately 400-500 nm, where zirconium starts to replace these two elements. This depth profile supports that ablation of the initial copper-silicon oxide layer was negligible and that laser irradiation induced the diffusion and partial mixing of the layer and substrate elements. Meanwhile, the Cu 2p and Cu LMM XPS spectra in Figure 3 reveals a mixture of Cu^+ and Cu^{2+} (1847.2 eV and 1850.6 eV of Auger parameter) species at the surface of the sample, in agreement with the previous assignments based on UV-vis measurements.

ii.- Laser irradiation within a laser furnace

Sample M4, prepared by annealing the precursor sample in a continuous roller furnace at 893 K, presents a UV-vis spectrum (Figure 6a)) characterized by an absorption band similar to that of sample M0. This renders a light greenish color that suggests the existence of large size copper oxide clusters.[14] The SEM analysis of this sample confirms that clusters with sizes ranging between 50-100 nm are randomly distributed onto a rather flat surface (Figure 6b)-left). The TOF-SIMS (Figure 6c)) depth profile of this sample reveals a regular and enriched distribution of Cu through an approximate depth equivalent to 800 s of sputtering, followed by another zone of about 100 s which, characterized by a decreasing Cu profile, indicates a certain diffusion of copper within the $ZrSiO_4$ substrate. Also, TOF-SIMS reveals an enrichment in silicon at the topmost surface layers. This elemental distribution suggests that both thermally induced melting and redistribution of elements occurred during the furnace treatment. We assume that furnace heating, followed by slow cooling, induces a surface melting and mixing of components that is accompanied by copper oxide agglomeration in clusters larger than those existing in sample M0. The diffusion of silicon (or the in-depth diffusion of copper) and the formation of an outer SiO_2 enriched thin layer was confirmed by a Si/Cu XPS ratio of 71.2 (Table 1). Meanwhile, the spectra in Figure 4 and the determined Auger parameters (1848.1 eV and 1851.0 eV, respectively, see supporting information S3) confirm that a majority of copper at the surface is in the form of Cu^{1+} and Cu^{0}, with a small Cu^{2+} contribution as deduced from the shape of the Cu2p peak.

Sample M5 was prepared by annealing the precursor sample in the furnace at 893 K while it was simultaneously irradiated with the CO_2 laser, as described in ref. [18]. This laser works in continuous mode and can be used to induce melting and atomic mixing with no significant incidence of ablation processes. The absence of ablation could be anticipated here by the very low irradiance values provided by this laser beam (see Table 1 and additional parameters in the supporting information Table S2). Sample M5 was highly reflective in the NIR (Figure 6a)), while its absorption bands in the visible at $\lambda < 650$ nm can be associated to absorption features of CuO (band gap of 1,2 eV) [4]. As a result of these spectral features, this sample presented a magenta color. The microstructure and cluster sizes between 50 and 100 nm observed by SEM (Figure 6b)-right) are similar to those found in sample M4, although particles at the surface adopted geometrical shapes with well-defined facets. The TOF-SIMS profile (Figure 6c)) of sample M5 is characterized by a rather homogenous but decreasing distribution of copper and zirconium up to a depth larger than 800 nm. This thick zone containing copper supports the occurrence of efficient melting and diffusion phenomena along the interface between the substrate and the Cu-SiO_2 coating layer. Such efficient diffusion can be accounted for by the existence of large temperature gradients through the depth of the induced melt where a Maragoni type convection and a vigorous liquid agitation before solidification through a vertical linear front are to be expected [29-31].

The XPS analysis of this sample reveals a little surface enrichment of Cu with a Si/Cu ratio of 18.2 and the absence of Zr at the surface. According to this analysis, copper is in the form of Cu2+ species (c.f. Figure 4) as revealed by an Auger parameter of 1850.9 eV.

Summary and conclusions

In this work we have developed a new method of coloring commercial ceramic tiles. It involves the MS coating of the tiles with Cu-Si mixed oxides, and the subsequent irradiation with NI (1064 nm) and CO_2 laser beams under different operating conditions, including a recently patented laser furnace apparatus. Appropriate adjustment of the laser irradiance and the processing temperature may induce different diffusion, melting/solidification, reduction, mixing, redeposition and ablation processes of the copper oxide and tile substrate materials. This gives rise to the appearance of grey, orange, magenta and dark green colors which are attributed to the prevalence of some of the following phenomena: (i) coating ablation accompanied by agglomeration of Cu nanoparticles, (ii) melting and mixing between the coating and the ceramic tile substrate, and (iii) efficient oxidation to copper oxide in continuous laser furnace experiments. All the described treatment rendered surface terminations of the ceramic tile with good adhesion and chemical resistance to acids as demonstrated by standardized tests. The reported panoply of treatments illustrates the possibilities of applying laser irradiation to MS deposition of oxide coatings for coloring ceramic tile components. The present work reports about the use of copper as transition metal cation, but the described procedure is compatible with other metals, which would open the way to the generation of a much wider set of colors.

Acknowledgements

Financial support from the EU (LIFE11/ENV/ES560), Innovaragón (ITA-DGA/ES 1368), DGA (Group T87), and projects 201560E055, MAT2015-69035-REDC and MAT2016-79866-R from MINECO are gratefully acknowledged. F. Rey-García acknowledges the Portuguese Science and Technology Foundation (FCT) for the Grant SFRH/BPD/108581/2015.

References

1. Pérez-Arantegui J, Larrea A, Molera J, Pradell T, Vendrell-Saz M. Some aspects of the characterization of decorations on ceramic glazes. Appl Phys A. 2004;79(2):235-9.
2. Stoyanova Lyubenova T, Peiró MC, A. R, Martí R, Calvet I, Carda JB. Synthesis of Ceramic Pigments by Non-Conventional Methods for New Ceramic Decoration Technologies. CFI-Ceramic forum international 2014.
3. Orera VM, Merino RI. Ceramics with photonic and optical applications. Boletin De La Sociedad Espanola De Ceramica Y Vidrio. 2015;54(1):1-10.
4. Chan GH, Zhao J, Hicks EM, Schatz GC, Van Duyne RP. Plasmonic properties of copper nanoparticles fabricated by nanosphere lithography. Nano Lett. 2007;7(7):1947-52.
5. Rico V, Lopez-Gascon C, Espinos JP, Lahoz R, Laguna M, Gonzalez-Elipe AR, et al. Metallization of ceramic substrates by laser induced decomposition of coordination complexes. J Eur Ceram Soc. 2016;36(11):2831-6.
6. Roque J, Molera J, Sciau P, Pantos E, Vendrell-Saz A. Copper and silver nanocrystals in lustre lead glazes: Development and optical properties. J Eur Ceram Soc. 2006;26(16):3813-24.
7. Imer C, Gunay E, Ovecoglu ML. Effects of firing temperatures and compositions on the formation of nano particles in lustre layers on a lead-alkali glaze. Ceram Int. 2016;42(15):17222-8.
8. Ocana M, Espinos JP, Carda JB. Synthesis, through pyrolysis of aerosols, of YIn1-xMnxO3 blue pigments and their efficiency for colouring glazes. Dyes Pigment. 2011;91(3):501-7.
9. Llusar M, Gargori C, Cerro S, Badenes JA, Monrós G. New Ceramic Pigments for the Coloration of Ceramic Glazes. In: Vincenzini P, editor. 13th International Ceramics Congress: Advances in Science and Technology; 2014. p. 148-58.
10. Jain A, Gonzalez CAE, Tejeda EM, Duran A, Contreras OE, Hirata GA. Covering the optical spectrum through different rare-earth ion-doping of YAG nanospheres produced by rapid microwave synthesis. Ceram Int. 2018;44(2):1886-93.
11. Guo D, Li LT, Cai K, Gui ZL, Nan CW. Rapid prototyping of piezoelectric ceramics via selective laser sintering and gelcasting. J Am Ceram Soc. 2004;87(1):17-22.
12. Lahoz R, de la Fuente GF, Pedra JM, Carda JB. Laser Engraving of Ceramic Tiles. Int J Appl Ceram Technol. 2011;8(5):1208-17.
13. Zhao XL, Evans JRG, Edirisinghe MJ, Song JH. Direct ink-jet printing of vertical walls. J Am Ceram Soc. 2002;85(8):2113-5.
14. Rico VJ, Lahoz R, Rey-Garcia F, Yubero F, Espinos JP, de la Fuente GF, et al. Laser Treatment of Nanoparticulated Metal Thin Films for Ceramic Tile Decoration. ACS Appl Mater Interfaces. 2016;8(37):24880-6.
15. Barranco A, Borras A, Gonzalez-Elipe AR, Palmero A. Perspectives on oblique angle deposition of thin films: From fundamentals to devices. Prog Mater Sci. 2016;76:59-153.
16. Kelly PJ, Arnell RD. Magnetron sputtering: a review of recent developments and applications. Vacuum. 2000;56(3):159-72.
17. Gil-Rosta J, Yubero F, Fernandez R, Vilajoana T, Artus P, Dursteler JC, et al. Colored semi-transparent Cu-Si oxide thin films prepared by magnetron sputtering. Opt Mater Express. 2011;1(6):1100-12.
18. Estepa Millan LC, De la Fuente Leis GF, inventorsContinuous Furnace with Coupled Laser for the Surface Treatment of Materials, US Patent 20090230105 (2009). China patent No. ZL 2012100224412 (2007). patent PCT/ES2007/070047. 2007.
19. Rey-García F, Gutiérrez-Mora F, Borrel CJ, Estepa LC, Angurel LA, De la Fuente GF. Microstructural characterization and tribological behavior of Laser Furnace processed ceramic tiles. Ceram Int. 2018;10.1016/j.ceramint.2018.01.133.
20. de Francisco I, Bea JA, Vegas A, Carda JB, de la Fuente GF. In-situ laser synthesis of Nd-Al-O coatings: the role of sublattice cations in eutectic formation. Acta Crystallogr Sect B-Struct SciCryst Eng Mat. 2015;71:95-111.

21. Eppler RA. ZIRCONIA-BASED COLORS FOR CERAMIC GLAZES. Am Ceram Soc Bull 1977;56(2):213-&.
22. Smith L, Cohen AJ. Absorption spectra of cations in alkali-silicate glasses of ultra-violet transmission. Phys Chem Glasses. 1963;4.
23. Espinos JP, Morales J, Barranco A, Caballero A, Holgado JP, Gonzalez-Elipe AR. Interface effects for Cu, CuO, and Cu2O deposited on SiO2 and ZrO2. XPS determination of the valence state of copper in Cu/SiO2 and Cu/ZrO2 catalysts. J Phys Chem B. 2002;106(27):6921-9.
24. Henley SJ, Carey JD, Silva SRP. Metal nanoparticle production by pulsed laser nanostructuring of thin metal films. Appl Surf Sci. 2007;253(19):8080-5.
25. Tahir D, Tougaard S. Electronic and optical properties of Cu, CuO and Cu2O studied by electron spectroscopy. J Phys-Condes Matter. 2012;24(17):8.
26. Bäuerle DW. Laser processing and chemistry: Springer; 2000 2000.
27. Schick HL. A thermodynamic analysis of the high-temperature vaporization properties of silica. Chem Rev. 1960;60(4):331-62.
28. Rubahn H-G. Laser Applications in Surface Science and Technology. New York, USA: John Wiley and Sons; 1996.
29. Kim YJ, Kou S. Thermocapillary convection in zone-melting crystal-growth - an open-boat physical simulation. J Cryst Growth. 1989;98(4):637-45.
30. Lennikov V, Ozkurt B, Angurel LA, Sotelo A, Ozcelik B, de la Fuente GF. Microstructure and Transport Properties of Bi-2212 Prepared by CO2 Laser Line Scanning. J Supercond Nov Magn. 2013;26(4):947-52.
31. Mora M, Diez JC, Lopez-Gascon CI, Martinez E, de la Fuente GF. Laser textured Bi-2212 in planar geometries. IEEE Trans Appl Supercond. 2003;13(2):3188-91.

Figure 1 MS experimental set-up: (1) silicon MS source, (2) copper MS source, (3) quartz crystal microbalance, (4) sample holder, (5) mass flow controllers, (6) pressure gauge, and (7) pumping system.

Figure 2 a) UV-vis-NIR transmittance spectra of the reference quartz sample as deposited. The inset presents normal SEM (left) and TEM cross section (right) ~~SEM~~ images of this precursor layer. Inset in the right side presents a high magnification TEM image of the interface between the precursor layer and the ceramic tile.

Figure 3 a) UV-vis-NIR total reflectance spectra of samples M0 and M1 and real photographs as insets. The insets show the color images of the tile samples. b) SEM images of the M0 (left) and M1 (right) samples. c) TOF-SIMS analysis of the time-evolution of the normalized Si^+, Cu^+ and Zr^+ signals in M0 and M1 samples.

Figure 4 Cu2p photoelectron (a) and Cu LMM Auger (b) peaks of the different samples analyzed by XPS. The red dot-slash lines are included to signal the characteristic features of the marked chemical species (see text). As reference, spectra of a cleaned Cu foil are also included.

Figure 5 a) UV-vis-NIR total reflectance spectra of samples M2 and M3 and real photographs as inset. The insets show the color images of the treated tiles. b) SEM images of the laser treated samples M2 (left) and M3 (right). c) TOF-SIMS analysis of the time-evolution of the normalized Si^+, Cu^+ and Zr^+ signals in samples M2 and M3.

Figure 6 a) UV-vis-NIR total reflectance spectra of samples M4 and M5 and real photographs as insets. The insets show the color images of the treated tiles. b) SEM images of the laser treated samples in vacuum M4 (left) and M5 (right). c) TOF-SIMS analysis of the time-evolution of the normalized Si^+, Cu^+ and Zr^+ signals in samples M4 and M5.

*Table I. Summary of laser irradiation and processing conditions, colors obtained, with their corresponding Hunter's parameters, and measured XPS Si/Cu ratios for the studied samples. *Power density.*

Sample	Temperature	Irradiance (MW/cm^{-2})	Color	Hunter's parameters (L* a* b*)			Si/Cu XPS ratio
M0	As deposited	---	Dark Green	89.3	-6.35	10.5	27.0
M1	298 K	12.7	Gray	85.3	1.87	3.90	5.3
M2	298 K	7.02	Gray	89.6	-0.51	6.92	8.6
M3	298 K	4.72	Orange	80.6	-2.44	27.4	22.1
M4	Laser Furnace 893 K	---	Greenish	89.8	-3.66	5.51	71.2
M5	Laser-Furnace 893 K	2.31x10^{-6}*	Magenta	55.8	11.1	3.49	18.2

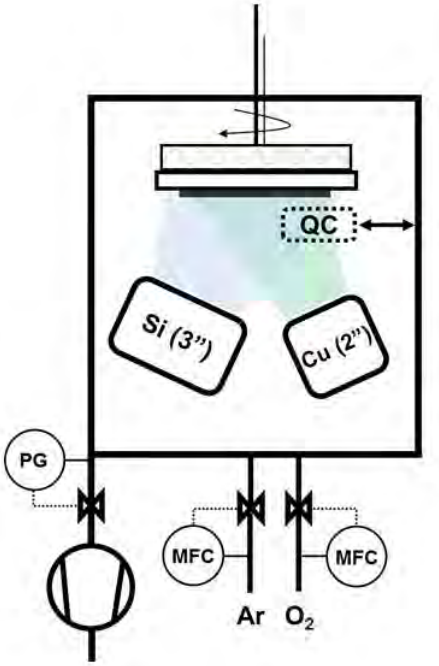
QC
Si (3")
Cu (2")
PG
MFC
MFC
Ar
O_2

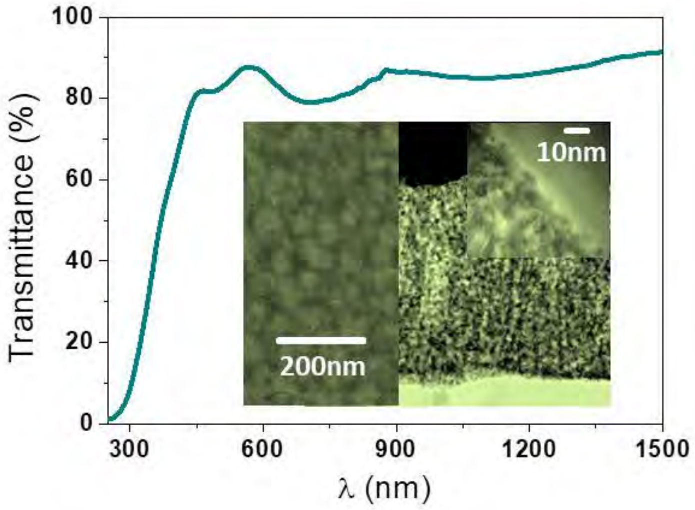
Transmittance (%)
100
80
60
40
20
0
300
600
900
1200
1500
λ (nm)
200nm
10nm

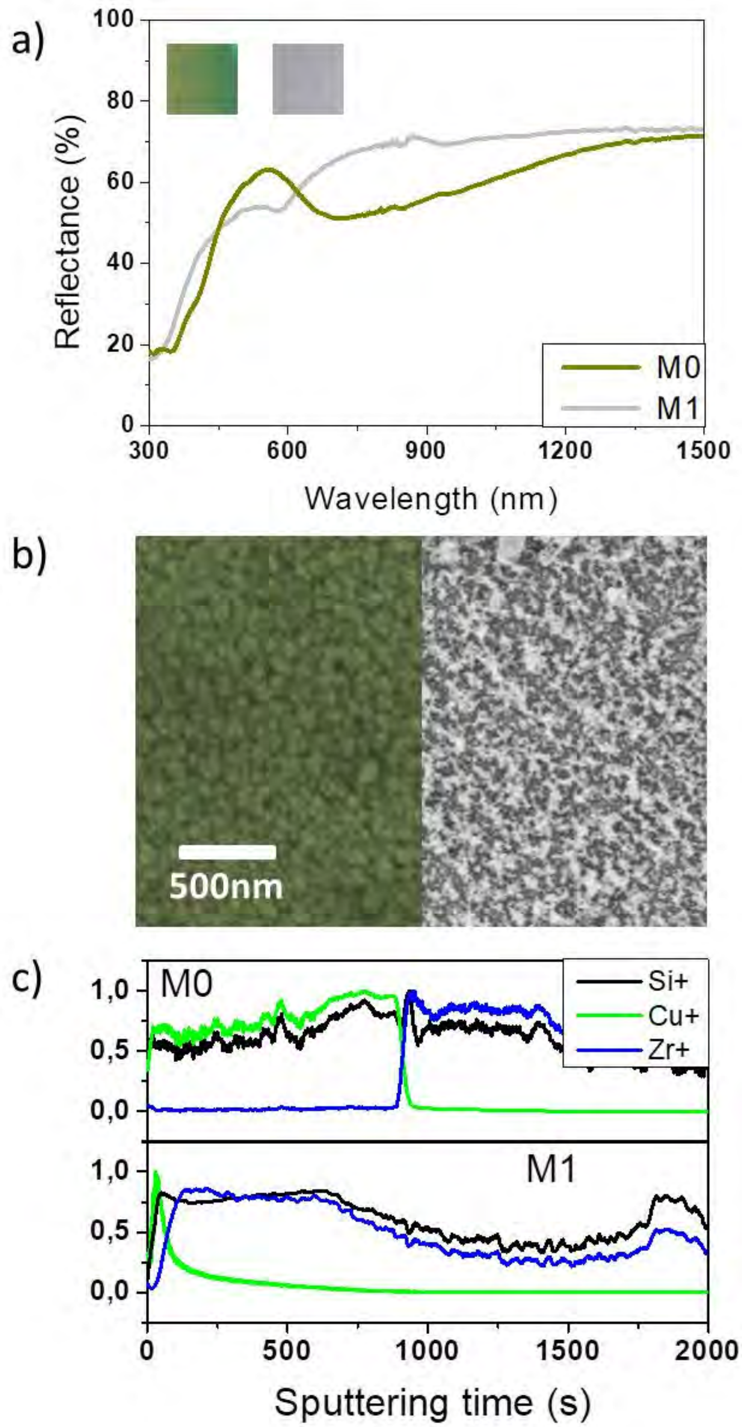
a)
Reflectance (%)
0
20
40
60
80
100
300
600
900
1200
1500
Wavelength (nm)
M0
M1
b)
500nm
c)
M0
M1
Si+
Cu+
Zr+
0,0
0,5
1,0
0
500
1000
1500
2000
Sputtering time (s)

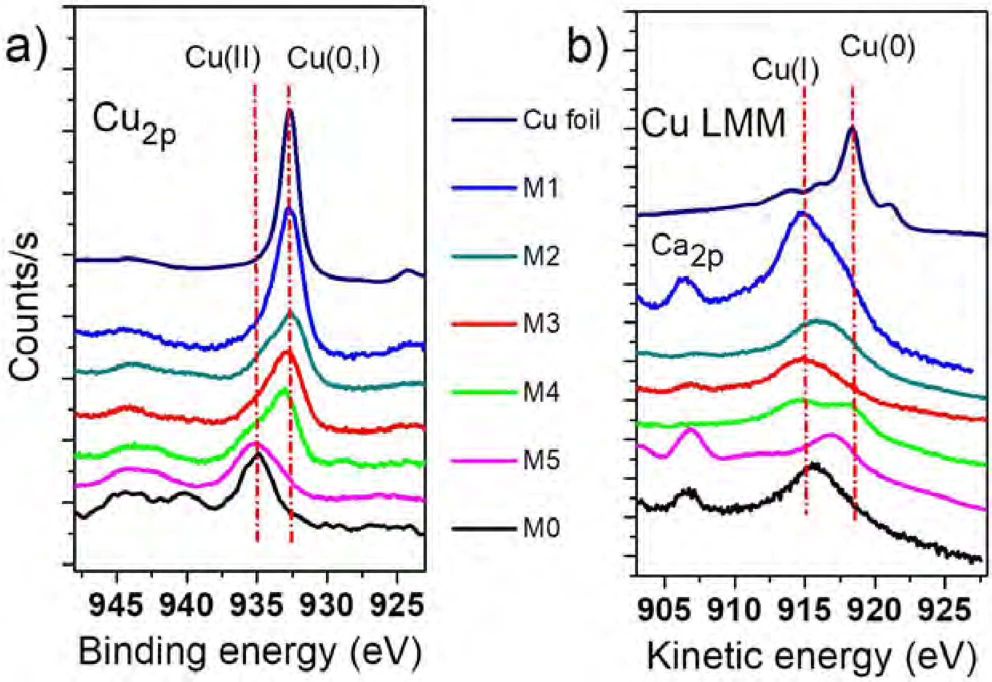
a)
Cu$_{2p}$
Cu(II)
Cu(0,I)
Counts/s
945
940
935
930
925
Binding energy (eV)
Cu foil
M1
M2
M3
M4
M5
M0
b)
Cu LMM
Cu(I)
Cu(0)
Ca$_{2p}$
905
910
915
920
925
Kinetic energy (eV)

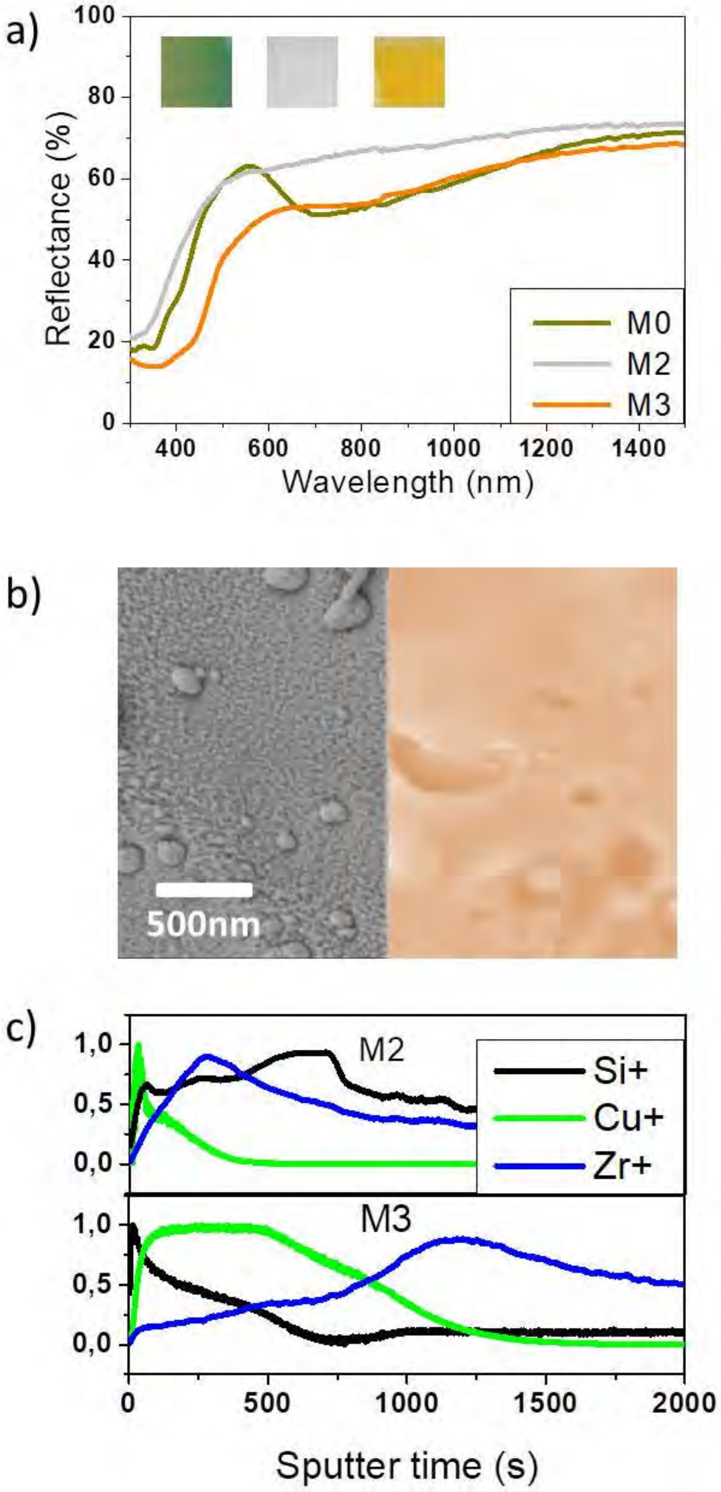
a)
100
80
60
40
20
0
Reflectance (%)
400
600
800
1000
1200
1400
Wavelength (nm)
M0
M2
M3
b)
500nm
c)
M2
1,0
0,5
0,0
Si+
Cu+
Zr+
M3
1,0
0,5
0,0
0
500
1000
1500
2000
Sputter time (s)

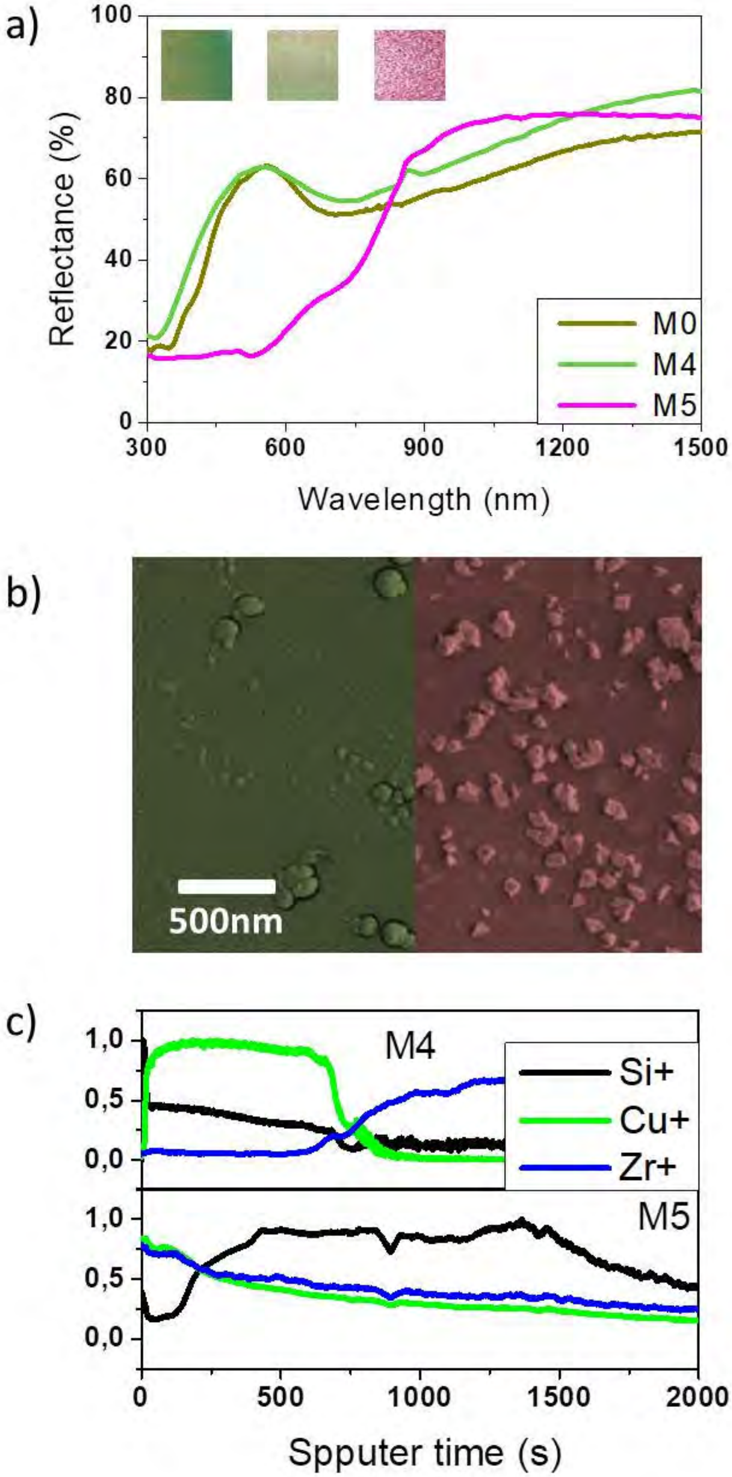
a)
100
80
60
40
20
0
Reflectance (%)
300
600
900
1200
1500
Wavelength (nm)
M0
M4
M5
b)
500nm
c)
M4
1,0
0,5
0,0
Si+
Cu+
Zr+
M5
0
500
1000
1500
2000
Spputer time (s)

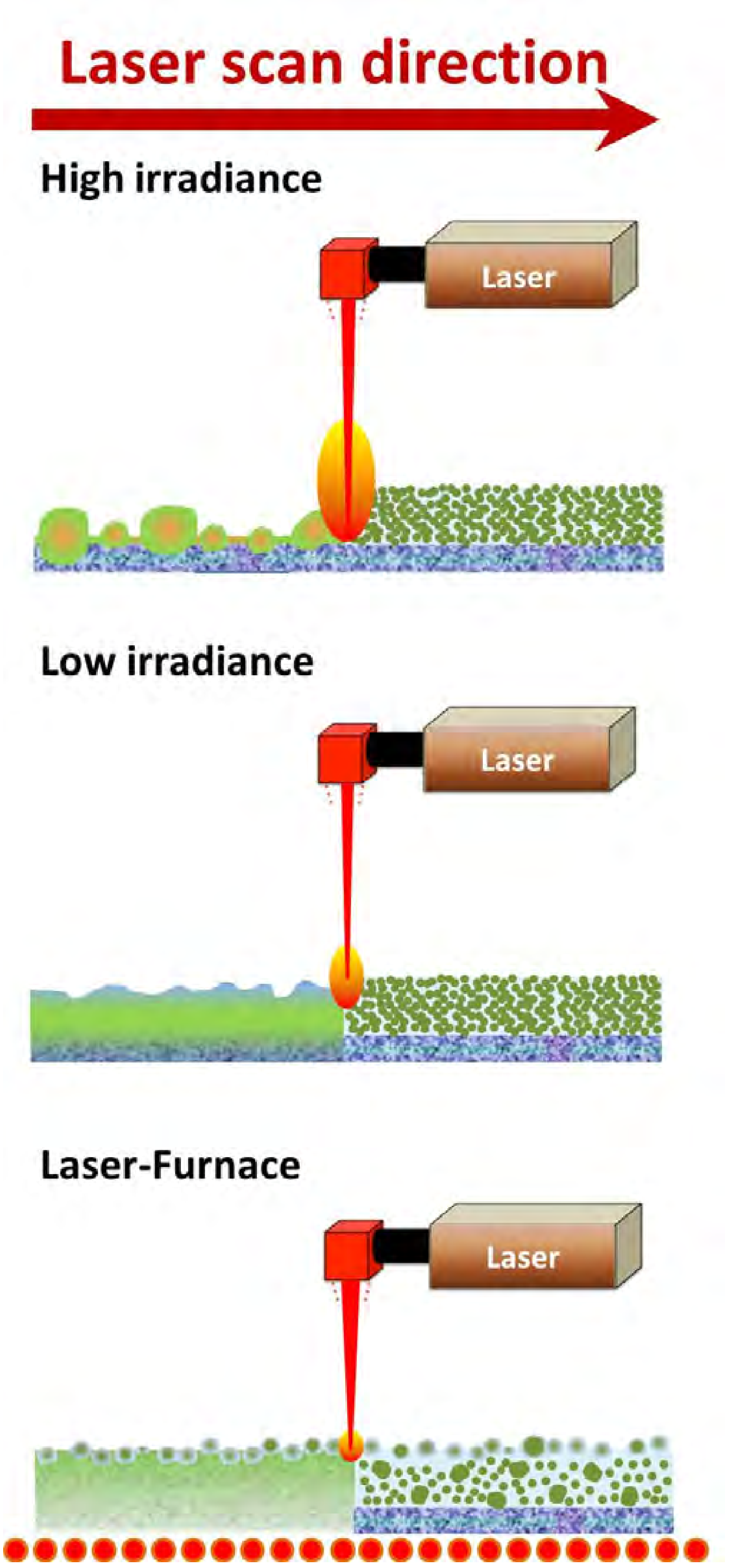
Laser scan direction
High irradiance
Laser
Low irradiance
Laser
Laser-Furnace
Laser